ASSESSMENT OF URBAN MICROCLIMATE OF THE SEMI-ARID CITY OF KANO, NIGERIA

By

Adewoye, A.R.*, Ukoha, A.P. and Okonkwo, S.J.

Remote Sensing of Tropical Ecosystem and Climate Change Modelling Group.
Forestry Research Institute of Nigeria
*Corresponding Author's Email: adewoye.ralph@frin.gov.ng

ABSTRACT

Kano is the largest city in Northern Nigeria with an estimated population of over 4 million inhabitants, the city is also an economic hub of Northern Nigeria. The activities within a city like Kano are known to change landscape structures and local climate activities. Urban forests are often planned by city planners to mitigate the alteration of microclimate arising from anthropogenic activities. Accurate and timely information is therefore needed on the microclimate of cities for the major purpose of improving the quality of life of urban residents. Remote sensing provides a straightforward and consistent way to determine thermal differences between distinct microclimate habitats arising from anthropogenic activities. This study used Satellite Remote Sensing to assess the varying microclimate temperatures occasioned by anthropogenic activities within the Kano metropolis. Kano City was divided into three strata, namely densely populated, sparsely populated, and urban forest. Land Surface Temperature was extracted from the 250 m Moderate Resolution Imagine Spectroradiometer's (MODIS) satellite images using JavaScript in the Google Earth Engine Platform. The extracted LST datasets were from March 2000 to September 2020. The datasets were analysed using Autoregressive Integrated Moving Average (ARIMA). Results showed that the densely populated areas had higher temperature ranges of 36.21°C, while the sparsely populated strata and the urban forested areas had 35.2°C and 34.4°C respectively. The study shows the impact of urban forestry in the reduction of microclimate heat and climate change mitigations. Monitoring the urban heat island in three areas of Kano City, an average of 4.88°C difference in temperatures between the urban forested areas and the densely populated areas of the city can be ascribed to the substitution of vegetation with buildings and hard surfaces and anthropogenic-induced heat generations.

Keywords: Climate change, Land surface temperature, Microclimate, Satellite remote sensing, Urban forest.

INTRODUCTION

Climate change fuelled by anthropogenic-induced forces is one of the most dangerous threats ever faced by humankind. The effects of climate change are converging in ways that threaten to have unprecedented negative impacts on urban quality of life, and socio-economic stability. These anthropogenic-induced changes are mainly due to population increase and infrastructural developments resulting in deforestation, urbanisation, agricultural expansion, etc. Urbanisation changes the physical energy balance of the environment through anthropogenically induced land use land cover changes (Tomlinson et al., 2011; Weng, 2012; Deng, 2013). Vegetated and permeable surfaces are changed into impermeable surfaces like roads buildings and parking lots. These urban infrastructures are made with steel and concrete, bitumen, and coal tares which have

higher heat retention capacities and low albedo and are responsible for creating a microclimate within an urban area (Owen et al., 1998, Xian & Crane, 2006, Hart & Sailor, 2009).

The urban thermal environment varies not only from its rural surroundings but also within the urban area due to intra-urban differences in land use and surface characteristics (Arthur-Hartranft et al., 2003; Hart & Sailor, 2009). Urbanisation transforms the natural landscape into anthropogenic urban land and changes surface physical characteristics thereby modifying the air temperature of the atmosphere (Voogt & Oke, 2003). Different surfaces possess diverse thermal differences, alter surface energy budgets, and directly affect urban climate; change in urban land surface temperature can have significant effects on local weather and climate (Bokaie et al., 2016; Alves & Lopez, 2017). In a simplified analogy, microclimate is simply comparing the temperature of the kitchen with that of an air-conditioned sitting room. Therefore, urban microclimate studies can be defined as the geographic delineation of various microclimates within an urban area determined by the transfers of energy, mass, and momentum at the city surface (Morgan et al. 1977).

Satellite remote sensing provides a straightforward and consistent way to determine thermal differences between distinct microclimate habitats arising from anthropogenic activities. Research studies into the relationship between microclimate and anthropogenic-induced changes have been widely carried out using Land Surface Temperature (LST). LST is the most fundamental criterion for establishing a linkage between surface changes and temperature changes. The availability of arrays of satellite remote sensing datasets has opened vistas of opportunities for the retrieved LST values from satellite data with various resolutions such as Landsat TM/ETM+ images 30 m, 120 m to 60 m (Owen et al., 1998, Arthur-Hartranft et al., 2003, Weng et al., 2004, Weng et al., 2005; Gluch et al., 2006), MODIS data 250 m, 500 m, and 1 km (Singh & Grover, 2014, Alavipanah et al., 2015; Wegmann et al., 2017; Ulpiani, 2020), and ASTER data (Tomlinson *et al*., 2011; Singh & Grover. 2014), and NOAA-AVHRR -1.1 km (Song et al. 2014; Ulpiani, 2020).

Kano is the largest city in Northern Nigeria with a population estimated to be above 4 million. The city is also an economic hub of Northern Nigeria. The anthropogenic activities within the city of Kano are changing the landscape structures and microclimate activities of the city. An important environmental issue that affects all major cities is the urban heat island effect. The costs and effects of increasing cooling on the ecosystem, as well as local increases in average yearly temperature, are widely established. The aggregation of urban heat island if unmitigated are likely to contribute to global warming. Accurate and timely information is therefore needed on the microclimate of cities to improve the quality of life of the urban residents, reduce the risk and cost associated with urban heat, and serve as an early warning system for urban developers and town planners. Such information is readily available with the aid of time series satellite remote sensing data sets. The study, therefore, used satellite remote sensing to assess the varying temperatures occasioned by anthropogenic activities within the Kano metropolis.

THE STUDY AREA

The study area is the metropolitan city of Kano, located in the savannah, south of the Sahelian region the Latitudes 11°54.55′ N - 12°04.09′ N and Longitudes 8°26.45′ E - 8°32.12′ E. Kano City has for centuries been the most important commercial and industrial nerve center of Northern (Nabegu, 2010; Abaje et al., 2014). The majority of the city's annual precipitation, which averages 690 mm, falls from June through September and the city is mostly very hot throughout the year, except for the months of December through February which is noticeably cooler (Nabegu, 2010; Mohammed, et al., 2019). The topography of the study area is an undulating plain underlain with basement complex rocks of Precambrian age, while the natural vegetation of the area is classified as Sudan savannah but has been transformed into a derived savannah region (Nabegu, 2010).

MATERIAL AND METHODS

As shown in Figure 1, the city was divided into three strata based on observed land cover types from the high-resolution Google Earth Pro; namely sparsely populated (SP), densely populated (DP), and urban forest (UF). Eight random points were selected for each of the delineated strata and the Land Surface Temperature (LST) dataset for the stratified areas was extracted from the Terra Land Surface Temperature and Emissivity 8-Day Global 1km (MOD11A2.006) using JavaScript on the Google Earth Engine (GEE) platform (*https://code.earthengine.google.com/*).

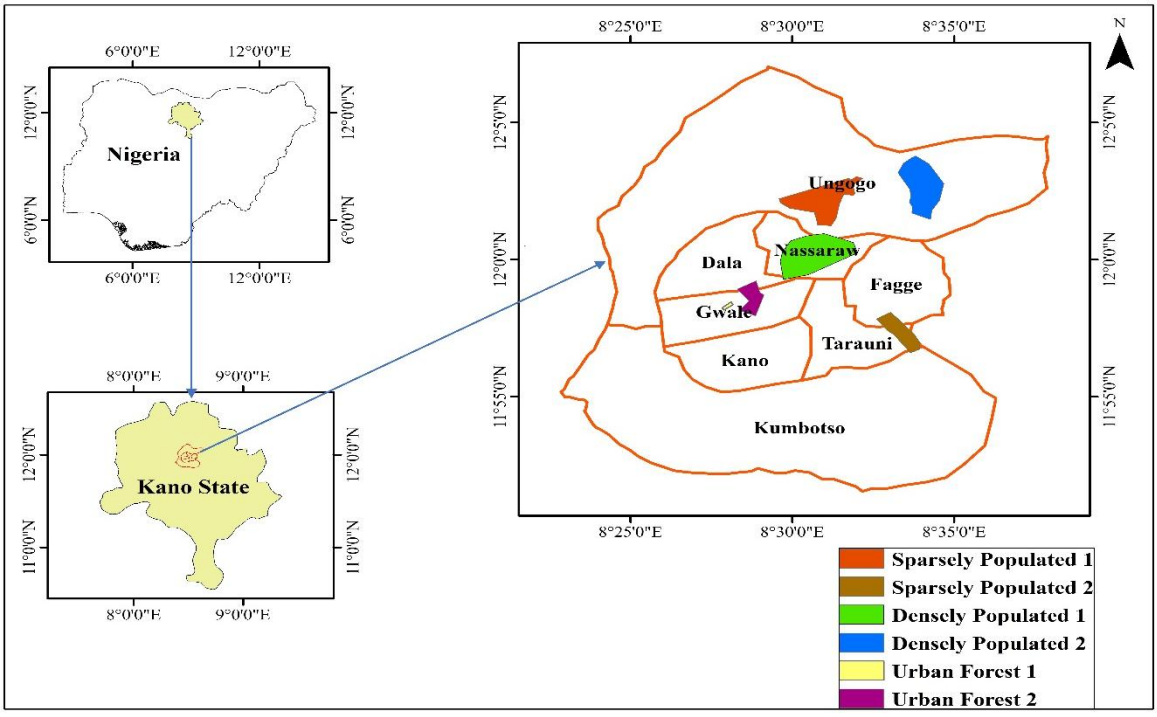

Figure 1: Map showing the delineated microclimates of the study area

The MOD11A2 .006 product provides an average 8-day land surface temperature (LST) in a 1200 x 1200 kilometer grid. Each pixel value in MOD11A2 is a simple average of all the corresponding MOD11A1 LST pixels collected within those 8 days. A pixel value covers 250-meter square, thus each of the random eight points is a representative of the 250 m^2 from the

delineated strata. The extracted LST datasets were from February 18, 2000, to August 28, 2020. The datasets were analysed using Autoregressive Integrated Moving Average (ARIMA). A cross-correlation coefficient was performed to measure the positive or negative strength among the six locations using Equation 1 below.

$R_{X_iX_j}(t_1, t_2) = E\left[X_{it_1}\overline{X}_{jt_2}\right]$--(1)

Let X_{it} and X_{jt} by two-time series variables of interest, where t is a time index, $X_{it}, X_{jt} \in R$, and $i, j \in Z$, such that $i \neq j$. Assuming each time series has means $\mu_{xi}(t)$ and $\mu_{xj}(t)$ respectively and variances $\sigma_{xi}^2(t)$ and $\sigma_{xj}^2(t)$ respectively at time t for each t, then the cross-correlation between the times t_1 and t_2 is defined as the expected value of both time series at the respective times t_1 and t_2. The Auto-regressive Moving Average (ARMA) was used to model the time series variables and predict future points in the variables. ARMA model forecasts variables that are time series by linearly combining their historic values (Dimri et al., 2020). ARMA model as a tool deals with all the aspects related to univariate time series model identification and its parameter estimation and forecasting ARMA model has the dual advantages of flexibility of use for modeling and its application to non-stationary time series data sets.

It is made up of the autoregressive part which is used to forecast time series variables by regressing it on a combination of its past values (Shumway & Stoffer 2017), and the integrated part which indicates the stationary of the time series data by subtracting the observations from the previous values (Lewis, *et al*. 2009), and the moving average part which uses the combination of errors in the past values to forecast future values (Becker. *et al*. 2004). Let $X(t)$ be the time series data of interest indexed by some set T, such that:

$$\{X(t) : t \in T\} \text{ ------------------------------------- (2)}$$

and $X_t \in R$. The ARIMA (p, d, q) model – where p is the order of the autoregressive part of the model (Shumway & Stoffer, 2017), d is the degree of differencing, and q is the order of the moving average part of the model – for the time series is given by:

$$(X_t - X_{t-1})^d + \emptyset_1(X_{t-1} - X_{t-2})^d + \ldots + \emptyset_p\left(X_{t-p} - X_{t-p+1}\right)^d = \varepsilon_t + \theta_1\varepsilon_{t-1} + \ldots + \theta_q\varepsilon_{t-q} \ldots\ldots (3)$$

Which is equal to:

$$\left(1 - \sum_{i=1}^{p} \emptyset_i\lambda^i\right)(1 - \lambda)^d X_t = \left(1 - \sum_{i=1}^{q} \theta_i\lambda^i\right)\varepsilon_t \ldots\ldots (4)$$

Where ε_t, $\emptyset_i$, θ_i, and λ^i represent the independently and identically distributed error terms of the model, the coefficients of the autoregressive part of the model, the coefficients of the moving average part of the model, and the lag operator respectively. When the time series is stationary, equation (3) becomes:

$$X_t - \emptyset_1 X_{t-1} - \ldots - \emptyset_p X_{t-p} = \varepsilon_t + \theta_1\varepsilon_{t-1} + \ldots + \theta_q\varepsilon_{t-q} \ldots\ldots (5)$$

Which is equal to:

$$X_t = \sum_{i=1}^{p} \emptyset_i X_{t-i} + \left(1 + \sum_{i=0}^{q} \theta_i\right)\varepsilon_{t-i} + k \ldots\ldots (6)$$

Where $\theta_0 = 1$, and k is a constant term. Equation (Mitchard, *et al*.) is known as the ARMA model. For each location, the derived LST time series observations were divided into a 70/30 ratio for training and validation.

Mean Absolute Percentage Error (MAPE)

$\boldsymbol{X_t}$ is the time series data of interest, where t is indexed from $\{1, 2, \ldots n\}$, and $X_t \in R$. $\boldsymbol{X_{t_{train}}}$ and $\boldsymbol{X_{t_{test}}}$ are subsets of X_t such that $(X_{t_{train}}, X_{t_{test}}) \in X_t$, then $X_{t_{train}}$ is such that $t_{train} = \{1, 2, \ldots, k\}$ and $X_{t_{test}}$ is such that $t_{test} = \{(k+1), (k+2), \ldots, n\}$. Also, let $X_{t_{pred}}$ be the forecasted values of X_t indexed from $\{(k+1), (k+2), \ldots, n\}$. The mean absolute percentage error (MAPE) is used to measure the accuracy of the forecasting method (De Myttenaere et al., 2015) and is expressed as:

$$MAPE = \frac{1}{(n-k)} \sum_{k+1}^{n} \left| \frac{X_{t_{train}} - X_{t_{pred}}}{X_{t_{train}}} \right| \quad \ldots\ldots (7)$$

Here, the absolute value in this calculation is summed for every forecasted point in time and divided by the number of fitted points n, multiplied by 100% making it a percentage error (De Myttenaere et al., 2015).

RESULTS AND DISCUSSION

Land Surface Temperature (LST) of Urban Densely Populated (UDP) areas was generally higher (35.74°C and 34.12°C) than LST from other locations, while the mean LST for the two sparsely populated areas was 31.84°C and 32.11°C respectively (Table 1). LST from urban forests (UF) was significantly lower at 28.5 and 31.6 degrees respectively. The forecast means for each of the locations using the ARIMA model with the MAPE test as shown in Tables 1 and 2 below is on the increase for the Densely Populated and the Sparsely Populated (SP1&2) temperatures, while the urban forest areas remain stable for both the dry and wet season.

Table 1: Mean temperature, the forecast means, and the accuracy-test results for each of the microclimate locations for the wet seasons

Locations	Mean	Forecast Mean	Mape Training	Mape Test
UDP 1	35.74	36.74	5.42	4.42
UDP 2	34.12	35.01	4.96	4.06
SP 1	31.85	32.73	4.10	4.29
SP 2	32.12	33.05	3.68	4.06
UF 1	28.50	28. 64	3.53	4.37
UF 2	31.68	31.62	3.75	4.14

Table 2: Mean temperature, the forecast means, and the accuracy-test results for each of the microclimate locations for the wet seasons

Locations	Mean	Forecast Mean	Mape Training	Mape Test
UDP 1	37.16	37.98	2.10	2.99
UDP 2	35.10	36.14	2.03	3.02
SP 1	29.06	30.18	3.09	3.75
SP 2	31.26	32.35	2.10	2.64
UF 1	26.95	27.0	2.75	3.45
UF 2	30.45	30.50	2.16	3.31

Observed mean temperature differences for the dry and wet seasons between the densely and sparsely populated, and the urban forests were significantly different (Tables 1 and 2). The lower mean temperature was observed within the urban forest areas, followed by the sparsely populated areas. While high mean temperatures were observed within the densely populated areas of the city. The graphs in Figure 2 and Figure 3 show average high-temperature ranges for the delineated areas of Urban Densely populated (UDP) within the dry and wet seasons.

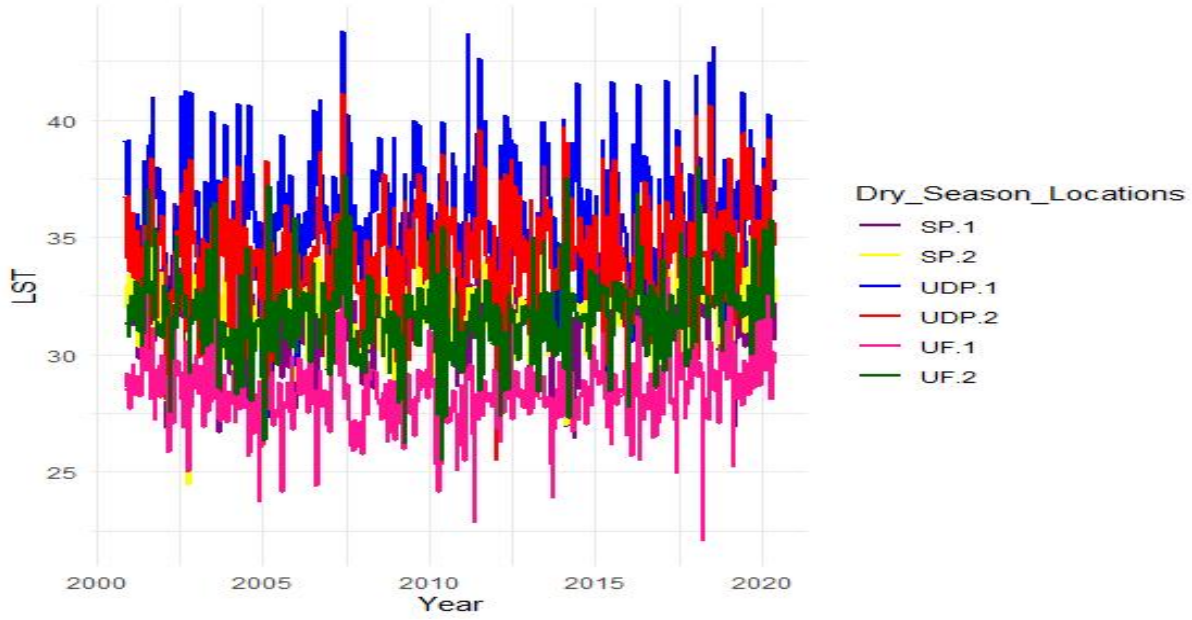

Figure 2: Dry season graph of Urban Densely Populated (UDP), Urban Sparsely Populated, and Urban Forest (UF)

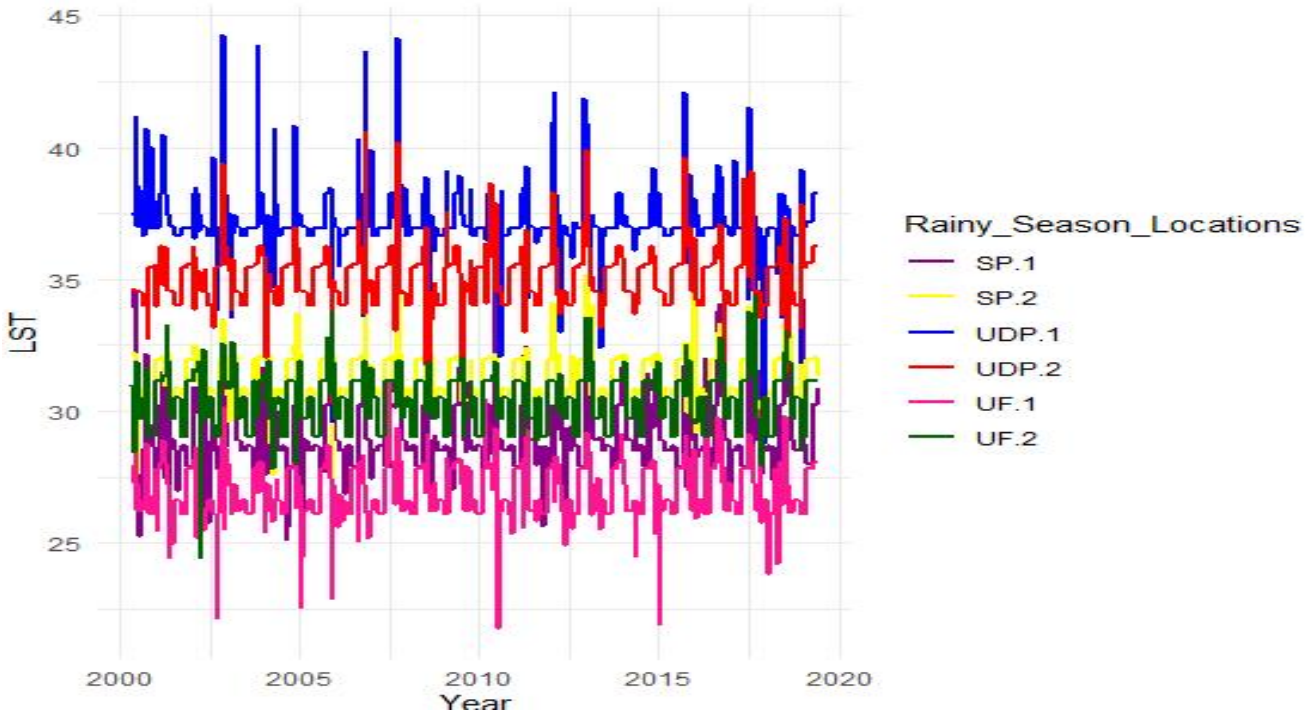

Figure 3: Dry season graph of Urban Densely Populated (UDP), Urban Sparsely Populated urban forest (UF)

Urban expansion in the form of housing and road construction is a direct impact of population increase and population increases, and the associated anthropogenic impacts have been on the rise within and around the city of Kano through urbanization. Urban expansion implies that paved roads and concrete buildings absorb and radiate more heat than vegetated areas (Singh and Grover, 2014).

Alteration of land surfaces occurs as a direct environmental effect of urbanisation. The implication of land modifications due to urbanisation is the development of impervious surfaces which makes up a sizable portion of the various developed lands (such as business, industrial, transportation, and residential lands). The physical characteristics of ground surfaces, such as soil moisture, material heat capacity, conductivity, albedo, and emissivity, among others, are altered as a result of this conversion, which lowers evapotranspiration (Shoshany et al., 1994; Friedl et al., 2002; Chudnovsky et al., 2004). The change in urban LST and atmospheric temperature, which has a significant impact on urban internal microclimatology, surface energy change, anthropogenic heat discharge, building energy consumption, atmospheric pollution, and human thermal comfort, is, therefore, one of the most significant environmental impacts (Deng & Wu, 2013).

Urban microclimates are known to respond to local land-cover composition and Land cover influences spatial distributions of LST. Vegetation covers are effective mechanisms of cooling as Urban vegetation is known to reduce heat islands through shading and evapotranspiration. Shading provided by Urban vegetation reduces the penetration of sunlight and reduces the energy storage in the soil and well-vegetated areas show lower air temperatures. Therefore, urban forest acts as heat absorbent by reducing air temperature by transpiration.

Continuous substitution of vegetation and green areas with artificial, impervious surfaces is one of the main humanly controlled factors that contribute to higher ambient urban air temperature (Tsoka et al., 2020). Monitoring the urban heat island in three areas of Kano City, an average of 5 ^{0}C difference in temperatures between the vegetated areas, ascribable to the substitution of vegetation with buildings and hard surfaces. In a similar study, Susca et al. (2011) observed a temperature difference of + 2 degrees centigrade between vegetated areas in New York City and other vegetated areas of the city. Also, previous studies have observed a positive relationship exists between LST and land cover types. Green Space or urban forest cover has heterogeneous patterns in air and land surface temperature that lead to cool refugia and warming hot spots within cities (Imhoff et al., 2010; Coseo & Larsen, 2014; Jenerette et al., 2016).

The planned areas of the city which are also the areas with urban forestry are usually reserved for inhabitants with high socio-economic status, while the densely populated and non-vegetated areas are places with low income/ socioeconomic status. For instance, a study by Huang and Cadenasso (2016) found a significant relationship between the urban heat island and socioeconomic factors. Higher Urban Heat Island (UHI) effects were linked to groups characterized by low income, high poverty, and less education. The inhabitants living within the Urban Densely Populated (UDP1 and UDP2) areas of the city are likely to be predisposed to infectious diseases. Life cycles of pathogens are influenced by the change in landscape or change in land use land cover and climate change indices such as rise in temperature (Wu et al., 2016; Tidman et al., 2021). Socio-economic status and population distribution also influence the spread of infectious diseases in humid tropics (Wilson, 2016; El-Sayed & Kamel, 2020).

Kano is a mega city and like most other African cities, socioeconomic status determines the habitation and living conditions of her inhabitants. One of the negative environmental and social consequences of urban heat is the spread of tropical communicable diseases such as diphtheria, Polio, and Meningitis. The incidence and spread of these diseases are often linked to rising temperatures (Bai et al., 2017). Research on the effect of meteorological factors on the incidence of *Meningococcal meningitis* observed that temperature increase was positively correlated with the incidence and spread of the disease. Akanwake et al. (2022) also noted that cerebral meningitis is a climate-sensitive disease, and its emergence and spread are associated with temperature rise.

CONCLUSION

Characterizing how urban forests and built-up land cover influence the microclimate of growing cities and their interrelationships with satellite remote sensing is an important research challenge in the 21st century. This study has clearly shown the influence of urban forests in regulating and mitigating temperature within Kano City. Remote sensing studies have shown that urban areas have unique environmental, climatic, and land use/cover characteristics as a result of intense anthropogenic activities. Consequently, urban areas have developed distinct microclimates and elevated temperatures and these microclimate components can have long-term impact on human health (Tsoka et al., 2020).

To mitigate the alteration of microclimate arising from anthropogenic activities, urban forests or green spaces are often planned with the city's landscapes. The major goal of climate adaptation efforts has been to cool cities and reduce UHI effects. Urban design and planning in warm, humid climates must take into account offering shade and ventilation in outdoor urban areas. Such steps can improve human comfort, protect human health, and reduce energy use.

Understanding the relationships between landscape compositions and LST is important for mitigating the urban heat island effect (Song et al., 2014). Therefore, mitigation of the UHI effects via the configuration of green spaces and sustainable design of urban environments has become an issue of increasing concern under changing climate. Accurate and timely information is therefore needed on the microclimate of cities to improve the quality of life of urban residents.

REFERENCES

Abaje, I.B., Ndabula, C. & Garba, A.H. (2014). Is the changing rainfall patterns of the Kano State and its adverse impacts an indication of climate change? *European Scientific Journal*, **10**(2), 1857- 7431.

Akanwake, J. B., Atinga, R. A. & Boafo, Y. A. (2022). Effect of climate change on cerebrospinal meningitis morbidities and mortalities: A longitudinal and community--based study in Ghana. *PLOS Climate,* **1**(8),1-16.

Alavipanah, S., Wegmann, M., Qureshi, S., Weng, Q. & Koellner, T. (2015). The role of vegetation in mitigating urban land surface temperatures: A case study of Munich, Germany during the warm season. *Sustainability*, **7**(4), 4689-4706.

Arthur-Hartranft, S. T., Carlson, T. N. & Clarke, K. C. (2003). Satellite and ground-based microclimate and hydrologic analyses coupled with a regional urban growth model. *Remote Sensing of Environment,* **86**(3), 385-400.

Alves, E. & Lopes, A. (2017). The Urban Heat Island Effect and the Role of Vegetation to Address the Negative Impacts of Local Climate Changes in a Small Brazilian City. *Atmosphere.* **8:** 1-14. 10.3390/atmos8020018

Bai, X., Hu, B., Yan, Q., Luo, T., Qu, B., Jiang, N., Liu J., & Y. Zhu (2017). Effects of meteorological factors on the incidence of meningococcal meningitis. *Afr Health Sci,* **17**(3), 820-826.

Becker, R., Walter, E. & Hurn, S. (2004). A general test for time dependence in parameters. *Journal of Applied Econometrics,* **19**(7), 899-906.

Bokaie, M, Z., Mirmasoud, K. A., Peyman, D., & Hosseini, A. (2016). Assessment of Urban Heat Island based on the relationship between land surface temperature and Land Use/ Land Cover in Tehran. *Sustainable Cities and Society*, **23:** 9-104. https://doi.org/10.1016/j.scs.2016.03.009

Chudnovsky, A., Ben-Dor, E. & Saaroni, H. (2004). Diurnal thermal behavior of selected urban objects using remote sensing measurements. *Energy and Buildings,* **36**(11), 1063-1074.

Coseo, P. and Larsen, L. (2014). How factors of land use/land cover, building configuration, and adjacent heat sources and sinks explain Urban Heat Islands in Chicago. *Landscape and Urban Planning*, **125:** 117-129.

Coulibaly, L., Migolet, P., Adegbidi, H.G., Fournier, R. & Hervet, E. (2008). Mapping above ground forest biomass from Ikonos high-resolution satellite image and multi-source geospatial data using neural networks and Kriging interpolation. *IEEE International Geoscience and Remote Sensing Symposium*. doi:10.1109/IGARSS.2008.4779342.

Deng, C., & Wu, C. (2013). Examining the impacts of urban biophysical compositions on surface urban heat island: A spectral unmixing and thermal mixing approach. *Remote Sensing of Environment,* **131:** 262-274.

de Myttenaere, A., Golden, B. Le Grand, B. & Rossi, F. (2016). Mean Absolute Percentage Error for regression models. *Neurocomputing,* **192:** 38-48.

Dimri, T., Ahmad, S. & Sharif, M. (2020). Time series analysis of climate variables using seasonal ARIMA approach. *Journal of Earth System Science,* **129**(1), 149.

El-Sayed, A. & Kamel, M. (2020). Climatic changes and their role in emergence and re-emergence of diseases. *Environmental Science and Pollution Research,* **27**(18), 22336-22352.

Friedl, M. A., McIver, J. C., Hodges, F., Zhang, X. Y., Muchoney, D. A., Strahler, H. C., Woodcock, E., Gopal, S. A., Schneider, A., Cooper, A., Baccini, A., Gao, F. & Schaaf, C. (2002). Global land cover mapping from MODIS: algorithms and early results. *Remote Sensing of Environment,* **83**(1), 287-302.

Gluch, R., Quattrochi, D. A. & Luvall, J. C. (2006). A multi-scale approach to urban thermal analysis. *Remote Sensing of Environment,* **104**(2), 123-132.

Hart, M. A. & Sailor, D. J. (2009). Quantifying the influence of land-use and surface characteristics on spatial variability in the urban heat island. *Theoretical and Applied Climatology,* **95**(3), 397-406.

Huang, G. & Cadenasso, M. L. (2016). People, landscape, and urban heat island: dynamics among neighborhood social conditions, land cover, and surface temperatures. *Landscape Ecology,* **31**(10), 2507-2515.

Imhoff, M. L., Zhang, P., Wolfe, R.E. & Bounoua, L. (2010). Remote sensing of the urban heat island effect across biomes in the continental USA. *Remote Sensing of Environment* **114**(3), 504-513.

Jenerette, G. D., Harlan, S. L., Buyantuev, A., Stefanov,W. L., Declet-Barreto, J. B., Ruddell, L., Myint, S.W., Kaplan, S., & Li, X. (2016). Micro-scale urban surface temperatures are related to land-cover features and residential heat-related health impacts in Phoenix, AZ USA. *Landscape Ecology,* **31**(4), 745-760.

Lewis, S. L., Lopez-Gonzalez, G., Sonke, B., Affum-Baffoe, K., Baker,T. R., Ojo, L. O., Phillips, O. L., Reitsma, J., White, M. L., Comiskey, J. A. Djuikouo, M. N., Ewango, C. E. N., Feldpausch, T. R., Hamilton, A. C., Gloor, M., Hart, T., Hladik, A. J., Lloyd, J. C. Lovett, J. R., … Woll H., (2009). Increasing carbon storage in intact African tropical forests. *Nature,* **457**(7232),1003-1006.

Mohammed, M.U., Hassan, N.I., & Badamasi, M.M. (2019). In search of missing link-Urbanisation and Climate Change Metropolis, Nigeria. *International Journal of Urban Sustainable Development*. **11**(3), 309-318.

Maimaitiyiming, M., Ghulam, A., Tiyip, T., Pla, F., Latorre-Carmona, Pedro, H., Ümüt, S., Mamat, C., & Mario, K (2014), Effects of green space spatial pattern on land surface temperature: Implications for sustainable urban planning and climate change adaptation. *SPRS Journal of Photogrammetry and Remote Sensing*, **89:** 59-66.

Mitchard, E. T. A., Saatchi, S. S., White, L. J. T., Abernethy, K. A., Jeffery, K. J., Lewis, L., Collins, M., Lefsky, M. A., Leal, M. E., Woodhouse, I. H. & Meir, P. (2012). Mapping tropical forest biomass with radar and spaceborne LiDARin Lop´e National Park, Gabon: overcoming problems of high biomass and persistent cloud. *Biogeosciences,* **9**: 179-191.

Morgan, D., Myrup, L., Rogers, D, & Basket, R.(1977). Microclimates within an Urban Area. *Annals of the Association of American Geographers,* **67**(1), 55-65.

Nabegu, A. B. (2010). An Analysis of Municipal Solid Waste in Kano Metropolis, Nigeria. *Journal of Human Ecology*, **31**(2), 111–119. doi:10.1080/09709274.2010.11906301 10.1080/09709274.2010.11906301

Owen, T. W., Carlson., T. N & Gillies., R. R. (1998). An assessment of satellite remotely-sensed land cover parameters in quantitatively describing the climatic effect of urbanisation. *International Journal of Remote Sensing,* **19**(9), 1663-1681.

Shoshany, M., Kutiel, P., Lavee, H. & Eichler, M. (1994). Remote sensing of vegetation cover along a climatological gradient. *ISPRS Journal of Photogrammetry and Remote Sensing,* **49**(4), 2-10.

Shumway, R. H. & Stoffer, D. S. (2017). *ARIMA Models. Time Series Analysis and its Applications: With R Examples*. Springer International Publishing**:** 75-163.

Singh, R. B. & Grover, A. (2014). Remote sensing of urban micro-climate with special Reference to Urban Heat Island island using Landsat thermal data. *GEOGRAPHIA POLONICA,* **87**(4), 14.

Song, J., Du, S., Feng, X. & Guo, L. (2014). The relationships between landscape compositions and land surface temperature: Quantifying their resolution sensitivity with spatial regression models. *Landscape and Urban Planning,* **123:** 145-157.

Susca, T., Gaffin, S. & Dell'Osso, G. (2011). Positive effects of vegetation: Urban Heat Island and green roofs. *Environmental pollution* (Barking, Essex: 1987), **159**: 2119-2126.

Tidman, R., Abela-Ridder, B. & de Castañeda, R. R. (2021). The impact of climate change on neglected tropical diseases: a systematic review. *Transactions of The Royal Society of Tropical Medicine and Hygiene,* **115**(2), 147-168.

Tomlinson, C. J., Chapman, L., Thornes, J. E. & Baker, C. (2011). Remote sensing land surface temperature for meteorology and climatology: a review. *Meteorological Applications,* **18**(3), 296-306.

Tsoka, S., Tsikaloudaki, K., Theodosiou, T. & Bikas, D. (2020). Urban Warming and Cities' Microclimates: Investigation Methods and Mitigation Strategies-A Review. *Energies* **13**(6), 1414-1438.

Ulpiani, G. (2020). On the linkage between urban heat island and urban pollution island: Three-decade literature review towards a conceptual framework. *Science of The Total Environment,* **751:** 141727.

Voogt, J. A. and Oke, T. R. (2003). Thermal remote sensing of urban climates. *Remote Sensing of Environment,* **86**(3), 370-384.

Weng, Q. (2012). Remote sensing of impervious surfaces in the urban areas: Requirements, methods, and trends. *Remote Sensing of Environment,* **117:** 34-49.

Weng, Q. & Larson, R. C. (2005). *Satellite Remote Sensing of Urban Heat Islands: Current Practice and Prospects. Geo-Spatial Technologies in Urban Environments*. Springer.

Weng, Q., D. Lu and J. Schubring (2004). Estimation of land surface temperature–vegetation abundance relationship for urban heat island studies. *Remote Sensing of Environment* **89**(4), 467-483.

Wegmann, M., Leutner, B. F., Metz, M., Neteler, M., Dech, S. & Duccio, R. (2017). A GRASS GIS package for semi-automatic spatial pattern analysis of remotely sensed land cover data. *Methods in Ecology and Evolution*. British Ecological Society.

Wilson, M. E. (2016). Geography of Infectious Diseases, *Infectious Diseases*. 938-947.e1. doi: 10.1016/B978-0-7020-6285-8.00106-4.

Wu, X., Lu, Y., Zhou, S., Chen, L. & Xu, B. (2016). Impact of climate change on human infectious diseases: Empirical evidence and human adaptation. *Environment International,* **86,** 14-23.

Xian, G. & Crane, M. (2006). An analysis of urban thermal characteristics and associated land cover in Tampa Bay and Las Vegas using Landsat satellite data. *Remote Sensing of Environment,* **104**(2),147-156.